

Parameter Sensitivity Visualization in DTI Fiber Tracking

Ralph Brecheisen, Bram Platel, Anna Vilanova, and Bart ter Haar Romeny

Abstract—Fiber tracking of Diffusion Tensor Imaging (DTI) data offers a unique insight into the three-dimensional organisation of white matter structures in the living brain. However, fiber tracking algorithms require a number of user-defined input parameters that strongly affect the output results. Usually the fiber tracking parameters are set once and are then re-used for several patient datasets. However, the stability of the chosen parameters is not evaluated and a small change in the parameter values can give very different results. The user remains completely unaware of such effects. Furthermore, it is difficult to reproduce output results between different users. We propose a visualization tool that allows the user to visually explore how small variations in parameter values affect the output of fiber tracking. With this knowledge the user cannot only assess the stability of commonly used parameter values but also evaluate in a more reliable way the output results between different patients. Existing tools do not provide such information. A small user evaluation of our tool has been done to show the potential of the technique.

Index Terms—Fiber Tracking, Parameter Sensitivity, Stopping Criteria, Diffusion Tensor Imaging, Uncertainty Visualization.

1 INTRODUCTION

Diffusion Tensor Imaging (DTI) is an imaging technique based on Magnetic Resonance (MR) that offers unique insight into the structural organisation of the brain white matter. This is accomplished by measuring the diffusion of water molecules in the tissue. In pure water this diffusion is characterized as *isotropic*, meaning that its magnitude is equal in all directions. In fibrous tissue however, the diffusion becomes restricted and shows a more or less distinct *anisotropy*, meaning that the diffusion magnitude depends on direction [4]. DTI involves measuring the diffusion magnitude in multiple directions for each point in the tissue. The magnitude distribution is then modelled as a 2nd-order tensor whose main eigenvector corresponds to the direction of greatest diffusion [2]. By tracing paths through the tensor field the underlying fiber structures can be reconstructed, a procedure that is called fiber tractography or fiber tracking [27, 20, 23]. Fiber tracking allows the white matter structures to be visualized and investigated in three dimensions. This is of great interest for the study of cerebral ischemia, neurodegenerative diseases and brain development but also for neurosurgical applications such as tumor resection and epilepsy surgery.

Despite its potential, the application of DTI fiber tracking in daily clinical practice remains limited. The main reason for this is a lack of understanding what the diffusion measurement actually quantifies. The notion that fiber structures are aligned with the direction of main diffusion is only an assumption and has not been completely validated. However, there are more reasons why acceptance of DTI fiber tracking is limited. The acquisition, processing and visualization of DTI data is fraught with uncertainties. Data acquisition suffers from signal noise, motion artefacts, partial volume effects and scan sequence parameters. In the case of DTI, the diffusion profile is assumed to be Gaussian and is modeled with a 2nd-order tensor. Such a model is an approximation of the true diffusion profile and is not valid in voxels containing multiple fiber orientations. Finally, the process of fiber tracking is a simplification of the data which is highly dependent on user input. Typical settings defined by the user are (1) the placement of seed points where tracking should start and (2) selecting the stopping criteria that determine when tracking terminates. It is unclear to

what extent the output of DTI visualization techniques is affected by the combined effect of all these uncertainties. Without showing these uncertainties any visualization of DTI data can potentially be misleading.

There has been a substantial amount of research on DTI visualization in the last few years. However, little attention has been paid so far to the visualization of uncertainties accumulated in the DTI processing pipeline. Even though the validation of DTI remains an open question, we believe that the acceptance of Diffusion Tensor Imaging in medical applications would be significantly improved if we find ways to show the different aspects of DTI uncertainty in a clinically relevant way. For this reason, we consider this to be the main focus of our research. In this paper, we concentrate on the uncertainties introduced by *user parameters*. Specifically, we look at the sensitivity of the fiber tracking algorithm with respect to the stopping criteria, that is, the threshold values that determine when fiber tracking should terminate. The two most commonly used stopping criteria are the *anisotropy threshold* and the *angular, angulation or curvature threshold*. The anisotropy threshold specifies that tracing should terminate if the anisotropy of the underlying tensor field drops below a certain value. There are different ways to compute the anisotropy of a tensor [27]. The curvature threshold specifies that tracing should terminate if the streamlines make curves that are too sharp. This threshold is primarily meant to deal with noise that would cause sudden directional changes within a voxel.

In many cases, a fixed set of thresholds is selected and re-used for different patient datasets. The threshold values are usually based on experience or empirical measurements of known anatomy. However, such measurements are not patient-specific. Furthermore, a small change in the threshold values can lead to very different output results. The user remains completely unaware of such effects and is therefore likely to either underestimate or overestimate the tracking results. Little or no effort is spent on evaluating the stability of the threshold values or what the effect of threshold variations is on the quantitative, tract-specific features that are commonly used in group studies (e.g. average fiber length or tract volume). If one is planning to draw conclusions based on such quantitative features, it is important to know whether the feature is sensitive to threshold variations or not. This has been recently confirmed in a clinical trial by Taoka et al. [26].

Different algorithms for fiber tracking exist, either based on line propagation or energy minimization [21]. We have chosen a line propagation algorithm based on streamline tracing, also known as the FACT algorithm (Fiber Assignment by Continuous Tracking) [20]. Because it is fast and simple to implement, it is the most widely used method for Diffusion Tensor Imaging. However, our visualization method is not limited to the FACT algorithm. The requirements we place on the algorithm are (1) that it makes use of stopping thresholds and (2) that variations in threshold values only affect streamline length. It should not affect streamline shape.

- Ralph Brecheisen, Anna Vilanova, and Bart ter Haar Romeny are with the Technical University Eindhoven, E-mail: {r.brecheisen,a.vilanova,b.m.terhaarromeny}@tue.nl
- Bram Platel is with the Maastricht Medical Center (Netherlands), E-mail: b.platel@tue.nl.

Manuscript received 31 March 2009; accepted 27 July 2009; posted online 11 October 2009; mailed on 5 October 2009.

For information on obtaining reprints of this article, please send email to: tvcg@computer.org .

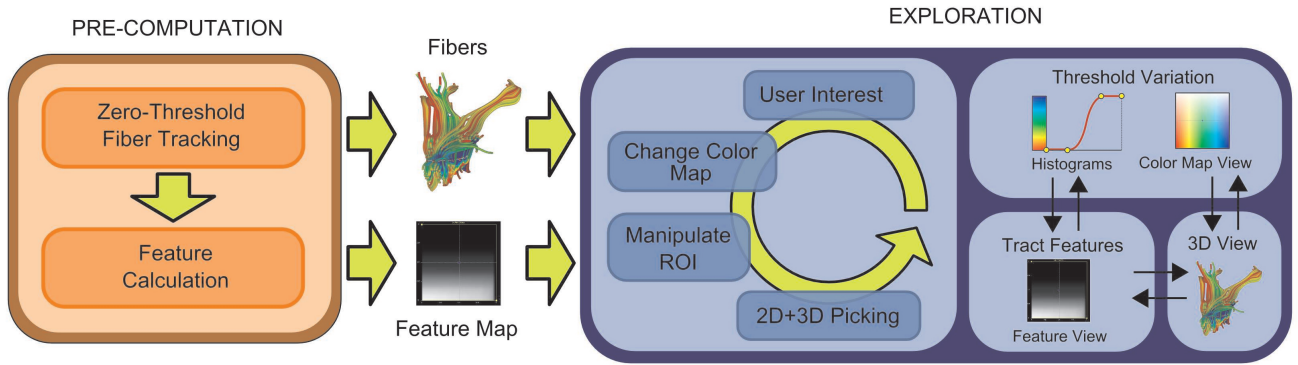


Fig. 1. Pipeline overview: (1) The pre-computation stage consists of two steps: Zero-threshold fiber tracking computes stopping criteria along streamlines. Tract feature calculation involves computing a quantitative metric for a discrete grid of sample points on the continuous parameter space. The feature values are stored in a feature map. (2) The exploration stage consists of tools and views to (i) investigate variations in the stopping criteria along the fibers and (ii) how these variations affect tract features such as the average fiber length. Selected threshold combinations can be picked in both 2D maps and 3D fiber view. Picking operations and manipulation of regions-of-interest are linked between the different views.

With existing fiber tracking tools, investigating how different threshold values in the stopping criteria affect the output results would require manually trying out many different threshold combinations. This is a very time-consuming process that may have to be repeated for every new dataset. Even if parameter values can be modified interactively, it would still leave the user wandering around blindly in an unknown parameter space. Furthermore, just seeing how a single parameter combination affects the output, is not sufficient. To give true insight into the algorithm's behavior across a *range of threshold combinations*, requires specific visualization techniques. To deal with these issues, we propose a visual exploration tool that allows users to investigate the behavior and sensitivity of DTI fiber tracking for stopping criteria. We will show that our tool can assist users to gain more insight into the sensitivity of the algorithm for these criteria. This should result in more reliable output results and an improved ability to compare groups of patients based on quantitative tract features. We also present a small user evaluation based on the experiences of three domain experts who use DTI fiber tracking on a regular basis in their own research.

The paper is outlined as follows: Section 2 reports on past research related to our work. Section 3 provides an overview of the processing pipeline of our tool. Section 4 describes the different pre-computation steps that are needed before exploration and visualization can start. Section 5 provides details on the different interaction features of our tool. In Section 6, we discuss the results of using our tool for studying parameter sensitivity in real datasets. We will also report on a short user evaluation we performed with three domain experts who use DTI fiber tracking on a regular basis. Section 7 finalizes the paper with conclusions and future work.

2 RELATED WORK

DTI fiber tracking [21] or fiber tractography [3] is not a specific technique but a collective name for different algorithms that reconstruct brain nerve fibers from diffusion-weighted MR data. Streamline tracing is the most widely used technique. The FACT (Fiber Assignment by Continuous Tracking) algorithm, which is used in this paper, was one of the first streamline tracing techniques [3, 8, 20]. However, other line propagation techniques exist such as the *tensorlines* algorithm where the full diffusion tensor is used to deflect the estimated fiber trajectory [31]. Once a set of fiber trajectories has been computed there are several ways of visualizing them, ranging from tensor glyphs, streamlines, streamtubes and hyperstreamlines [27]. The latter uses all three eigenvectors and eigenvalues to shape the cross-section of the tube.

Most streamline tracing techniques use the eigenvectors of the diffusion tensor to estimate the direction of white matter fibers. However, due to noise there is a considerable uncertainty involved in the

calculation of the eigenvectors. Small errors are made at each step of the path propagation so that the total accumulated error can be quite large, possibly leading to incorrect pathway reconstructions. Several authors have investigated directional uncertainty in DTI fiber tracking from a mathematical viewpoint [14, 16]. However, the *visualization* of uncertainty in DTI fiber tracking has received less attention. Some efforts have been made in the past to visualize uncertainty in vector fields [6, 17, 22, 33] and surfaces [12, 18]. However, specific uncertainty visualization techniques for DTI fiber tracking are not widely available, despite reports on the need for such visualizations in neurosurgery [30].

One source of uncertainty in DTI visualization that has not received much attention is *parameter sensitivity*. Fiber tracking algorithms are highly dependent on user-defined parameters and this results in a poor reproducibility of the output results. Some reproducibility studies have been reported [7, 28], however there does not exist an automatic solution that resolves the problem for each dataset. This is where visualization can play an important role. However, sensitivity to input parameters is not limited to fiber tracking and can be observed in other user-guided algorithms as well, such as image registration or segmentation. Only a few attempts have been reported to visualize the variability in the output of such algorithms as a result of parameter changes. Hadwiger et al. [13] apply this concept to feature detection and quantification in industrial CT data. They perform region growing segmentation on the CT data for many different combinations of input parameters, thereby obtaining a complete space of output results that is subsequently visualized interactively. Our work uses a similar approach by applying this "parameter-space" concept to DTI streamline tracing.

The method we propose for investigating parameter sensitivity is based on generating a streamline superset that covers the whole parameter space of stopping criteria, and then using selective culling to display only specific streamline collections. This is an approach similar to Wei et al. [29], Doleish et al. [10] and Wenger et al. [32], even though they are not specifically focussing on parameter sensitivity. Furthermore, the tract features we define, such as average fiber length or average fiber density per voxel, are similar to the tractography metrics used in population (comparative) studies as discussed by Correia et al. [9].

3 PIPELINE OVERVIEW

An overview of our processing and exploration pipeline is illustrated in Figure 1. The pipeline consists of two main stages: (1) an unattended pre-computation stage, and (2) an exploration stage where the user visually explores the results of the pre-computation stage. The pre-computation stage (Section 4) consists of generating streamlines for the full space of threshold values. In Section 4.1 we explain in more

detail how these results can be computed in a fast and simple manner. We also compute a number of quantitative *tract features* on a grid of sample points in the threshold space (Section 4.2). This results in a feature map that allows the user to see the effect of threshold variations on such features. Finally, the exploration stage provides a number of views and interaction tools to visually explore threshold variations and their effect on tract features.

4 PRE-COMPUTATION

The pre-computation stage generates the information to interactively explore the threshold variations in fiber tracking. The only user-defined settings required at startup are the geometry of the seed region and which anisotropy measure to use (fractional, linear, etc.). However, our approach is not restricted to the use of seed regions. It is possible to perform whole-brain fiber tracking and then select a subset of fibers to be investigated [1, 5].

4.1 Zero-Threshold Fiber Tracking

The basis for our exploration pipeline is the theoretical set of fiber bundles or *fiber tracts* resulting from streamline tracing with all possible combinations of threshold values. Once we have this set of tracts, we can visualize them interactively, compute tract features and show how the feature values change as we modify threshold values.

A fast and simple way to obtain the required tracking results for the whole space of threshold combinations is to perform so-called *zero-threshold* streamline tracing, meaning that we allow tracing to proceed in an uninhibited manner without thresholds. We do this only once for a given seed region and this results in a collection of streamlines with maximum length and maximum curvature, the so-called *zero-threshold tract*. While performing zero-threshold tracing, we inspect the local tensor anisotropy and curvature in each streamline point and store, as additional point attributes, the combination of threshold values that would have terminated tracing at this point. This approach works because the thresholds we are considering only affect streamline *length*, not shape. Figure 2 illustrates the concept of zero-threshold tracking for the anisotropy threshold. As can be seen in the graph the anisotropy along the fiber is not always monotonically decreasing. The anisotropy *threshold* on the other hand, by definition, is always monotonically decreasing. After all, once the anisotropy drops below the threshold, streamline tracing terminates regardless of whether there are higher anisotropy values further along the fiber. The same exact reasoning holds for streamline curvature and the curvature threshold. To visualize specific output results for a given threshold combination we apply a simple filtering procedure on the streamline points of the zero-threshold tract. Streamline points with threshold values *above* the selected threshold combination are simply discarded.

4.2 Calculation of Quantitative Tract Features

DTI fiber tracking is most widely used in population studies that require statistics to show abnormalities in either brain or muscle tissue (e.g. in the heart). To be able to quantitatively compare fiber tracking results between patients and healthy controls, users often define so-called tract features (also called tract metrics) that compute some property of a given fiber tract or muscle. Examples are total and average fiber length [9].

A general problem of such quantitative features is their dependence on fiber tracking parameters such as the stopping criteria. It is important to check whether a particular tract feature remains stable for any threshold variations, and if so, for which regions of the threshold space this holds. The anisotropy and curvature threshold combinations we are considering in this paper span a continuous 2D space. Obviously we cannot compute a tract feature for each point in this space since there are infinitely many of them. We can however define a regular grid of sample points and compute tract features for those. We call such a grid of computed feature values a *feature map* and it allows us to visualize how a given tract feature varies as a function of threshold combination. In the following paragraphs, we will discuss a number of tract features that we implemented in our tool. This list is by no means complete since many different,

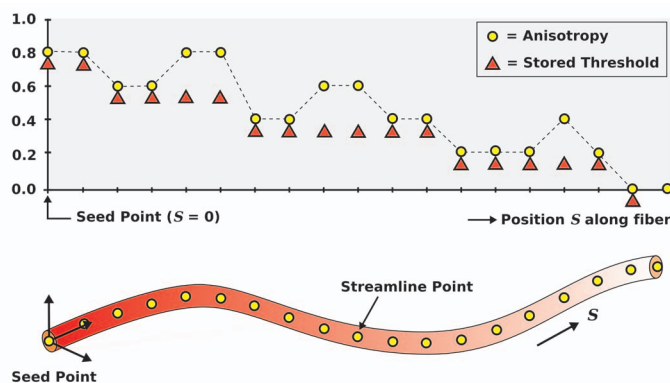


Fig. 2. Anisotropy threshold profile along single example fiber starting from the fiber seed point on the far left. The yellow circles indicate the variation of tensor anisotropy along the fiber. The orange triangles indicate the anisotropy threshold that is stored for each point. As can be seen, the anisotropy itself does not need to be monotonically decreasing. The threshold value is always monotonically decreasing. The same holds for streamline curvature and curvature threshold.

application-specific tract features can be defined. In principle, our tool can be extended with any scalar-valued tract feature that can subsequently be analyzed for stability.

Total, Average and Standard Deviation Fiber Length These tract features are the most widely used. Correia et al. [9] define as many as nine different tract features based on fiber length, each tuned for specific white matter conditions. For example, old age is generally accompanied by a significant reduction in both total and average fiber length. In conditions where fiber anisotropy is interrupted by multiple lesions, the total fiber length may not differ from a healthy person. The average fiber length however may reveal this condition quite clearly.

Average Fiber Density per Voxel We compute this feature by counting, for each non-empty voxel, the number of streamlines intersecting that voxel. The total count is then divided by the number of non-empty voxels to obtain the average fiber density. Of course, this feature depends on both dataset resolution and seed point density. However, this is not problematic, because for analyzing feature stability we are only looking for changes (or lack thereof) in single dataset. In certain compact and elongated fiber tracts (such as the cingula or optic radiations) the streamlines remain closely packed together. If at some threshold values the streamlines start running off in random directions we expect the average fiber density per voxel to drop.

Tract Volume This is another popular tract feature whose reduction can point to neurodegenerative diseases such as Alzheimer's. In studies of muscle tissue, tract volume can be used, together with average fiber length, to create models of specific muscles for biomechanical simulations. Tract volume can be computed by taking the volume of a single voxel and multiplying this by the total number of non-empty voxels. It is also possible to take the fiber density of each voxel into account as a weighting factor.

Mean of End-Point Distances We derived this feature from the area of fiber clustering. In fiber clustering you start with a single fiber and try to find neighboring fibers that look similar according to some similarity measure. In this case, we already have a cluster (a single fiber tracking result) and we wish to compute the average similarity between its streamlines. The average of end-point distances is a similarity measure adapted from Moberts et al. [19]. Fibers are considered to be similar if they have end-points that lie close together. This reflects the fact that fibers from the same anatomical structure connect

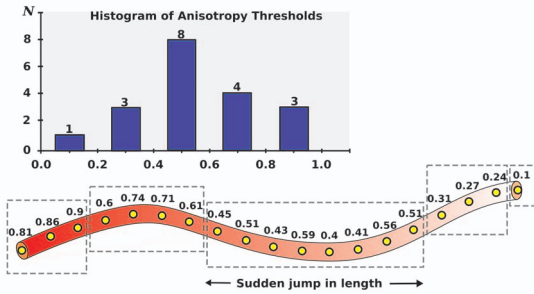


Fig. 3. Histogram of continuously varying anisotropy thresholds along single fiber. The peak between $[0.4 - 0.6]$ corresponds to a sudden jump in fiber length indicating a possibly critical threshold value.

the same areas of the brain. The end point distance d_E between fibers F_i and F_j is defined as,

$$d_E = \min(d_1, d_2) \quad (1)$$

where,

$$d_1 = \|F_{i,1} - F_{j,1}\| + \|F_{i,end} - F_{j,end}\| \quad (2)$$

$$d_2 = \|F_{i,1} - F_{j,end}\| + \|F_{i,end} - F_{j,1}\| \quad (3)$$

Here, $F_{i,1}$ and $F_{i,end}$ refer to the first and last points on fiber F_i . The end-point distances are computed for each fiber pair and averaged for the given tract. This is then repeated for all threshold combinations.

4.3 Cumulative Histograms

In addition to the feature map we also provide a number of histogram views as an alternative way to show the variation of threshold values along streamlines and the stability of tract features within the threshold space. To make it easier to detect stable regions, the histograms can be viewed as cumulative distributions.

Threshold Histograms If we consider the zero-threshold tract that was computed in the pre-computation step (Section 4), we can create a two-dimensional threshold histogram by subdividing the threshold space into bins. We can then assign each streamline point in the zero-threshold tract to its corresponding bin according to the threshold values stored at this point. Technically, the 2D histogram is not the same as a feature map but we can use the feature map view to display this 2D histogram. We can also compute a histogram for each threshold separately. This is illustrated in Figure 3 for the anisotropy threshold. A peak in the histogram corresponds to a sudden jump in overall fiber length, possibly pointing to a critical combination of threshold values. An alternative approach to obtain a 2D histogram is to normalize the individual 1D histograms and adding them multiplicatively to form a 2D joint probability distribution. This would assume however that anisotropy and curvature are independent variables, which need not be the case. As Figure 4 illustrates it is quite reasonable to believe that the average anisotropy in a voxel depends on the average curvature of fibers.

Feature Histogram The feature histogram provides an alternative view on the distribution of feature values in the threshold parameter space. The user can choose whether to show a normal histogram or the cumulative distribution. As explained in Section 4.2 this can help detect stable regions where threshold changes have little effect.

5 EXPLORATION OF THRESHOLDS AND TRACT FEATURES

After the pre-computation stage has finished the user can start to interactively explore threshold variations and their effect on different tract features. For this purpose, we provide a 3D view for displaying streamline output, 2D plots capturing the threshold space and allowing the user to select and manipulate threshold ranges interactively, and

quantitative histograms for detecting stable regions in the feature map. The different elements of our tool's user interface (shown in Figure 5) are described in the following paragraphs.

3D Viewing and Interaction: In the upper-left of Figure 5 the 3D view is shown where the different tracking results can be visualized. The fibers can be represented either by streamlines or streamtubes. Each vertex on the streamline or streamtube is associated with a set of threshold values calculated in that vertex and which are stored as 2D texture coordinates. This allows us to use 2D texture mapping to apply different color maps to the fibers. We also provide the option to map one threshold parameter (e.g., curvature threshold) to the radius of a streamtube and the other to color. If the user finds color transitions on the fibers that may point to interesting threshold changes, he or she can pick specific points on the fiber and see in the color map view (described next) what the exact threshold value is in that location.

Color Map View: Although this view is also used to display the color map that is currently active, it is primarily meant as an interaction tool. It allows the user to pick points in the 2D threshold space and immediately see what the fiber tracking result would be in the 3D view. In this case, the color map is applied to the full range of threshold values ($[0, 1] \times [0, 1]$). For example, an anisotropy threshold of zero is mapped to a red color, while an anisotropy threshold of one is mapped to a blue color with intermediate values going through white. However, if the user wishes to study variations in the local Region-Of-Interest (ROI) surrounding a given threshold combination, the color map should be applied to this region only. Figure 6 shows the relation between ROI selection and fiber coloring/geometry. The color map view allows the user to specify such a ROI, and move/resize it interactively with immediate updates in the 3D view. Figure 7 illustrates how ROI coloring improves the distinction between threshold variations along the fibers.

1D and 2D Color Maps: We support a number of uni- and bivariate color maps to highlight threshold variations along the fibers, either to show the anisotropy threshold, curvature threshold or both. There has been a substantial amount of research in the area of uni- and bivariate color mapping [25, 24]. Figure 9 shows the different color maps we support. Gray scales are well suited for detecting subtle changes in value and preserves the order of data values. For this reason we use it primarily to highlight tract feature values. Double-ended color scales specifically highlight low, medium and high values which make them effective for visualizing threshold variations. This is quite effective in combination with defining a ROI in the color map view because the ROI focusses the center and extrema of the color scale to a smaller threshold range. The 2D complementary color scale is defined by colors that lie on opposite sides of the hue circle. For example, one variable X of range $[X_{max} - X_{min}]$ is mapped to brightness of green. Another variable Y of range $[Y_{max} - Y_{min}]$ is mapped to brightness of the complementary color, which is purple [11]. The contribution of both variables is obtained by adding the colors in RGB space. This color scale highlights the absence or presence of correlations between two variables [25, 24]. As explained in Section 4.2 there may exist a correlation between curvature and anisotropy. However, when we

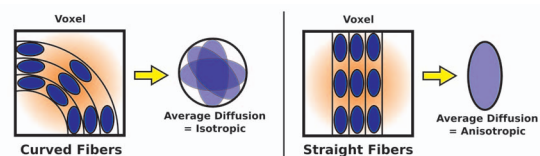


Fig. 4. Example of possible correlation between curvature and anisotropy. High curvature inside a voxel averages anisotropies with different orientations, which may result in a measurement with (near) isotropic diffusion. Zero curvature in a voxel with the identical anisotropy values results in greater average anisotropy.

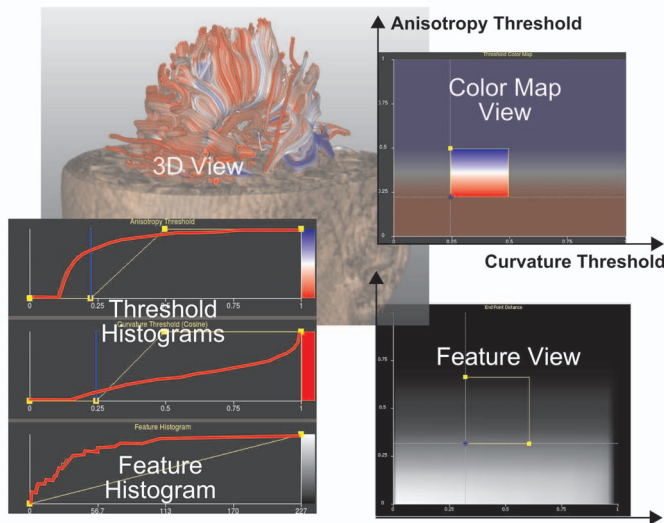


Fig. 5. Main viewports of our exploration tool. Top-left: 3D visualization of fiber tract together with anatomical context and axial fractional anisotropy slice. Top-right: color map view used for selecting individual threshold combinations and definition of color detail regions. Bottom-right: feature map view showing changes in quantitative tract features as a function of threshold combination at discrete sample points of the parameter space. Bottom-left: cumulative histograms of both threshold and feature values.

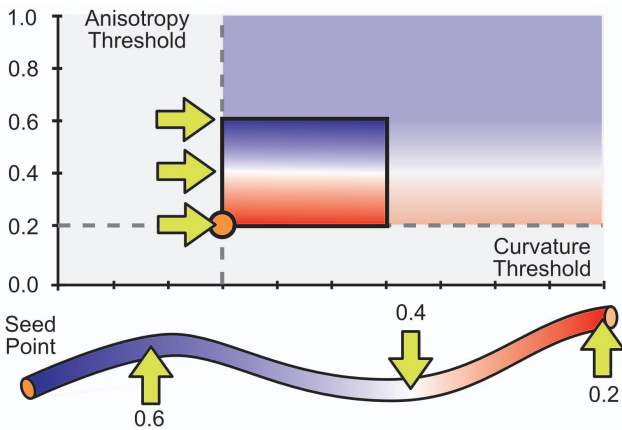


Fig. 6. Relation between region-of-interest (ROI) selection and application of color map to subrange of threshold values. The streamlines displayed in the 3D view correspond to lower-left corner point of the ROI. The color mapping along the streamlines would show how they shorten due to increasing threshold values.

applied this color scale to the fibers this correlation was not visually detectable.

Two color scales remain, namely the 1D hue color scale and the 2D hue-saturation color scale. Despite its limitations, hue remains one of the most popular and widely used color scales. It is difficult to interpret without the use of a color legend and the scale introduces discontinuities that may not be present in the data itself. Nevertheless, we include it for completeness. The 2D hue-saturation scale suffers from similar drawbacks, even though the problem is somewhat alleviated if we link hue to curvature threshold (which varies much less than the anisotropy threshold). Saturation has similar properties as the gray scale but when combined with hue it loses contrast and is less effective for detecting changes.

Feature Map View: When DTI fiber tracking is applied in

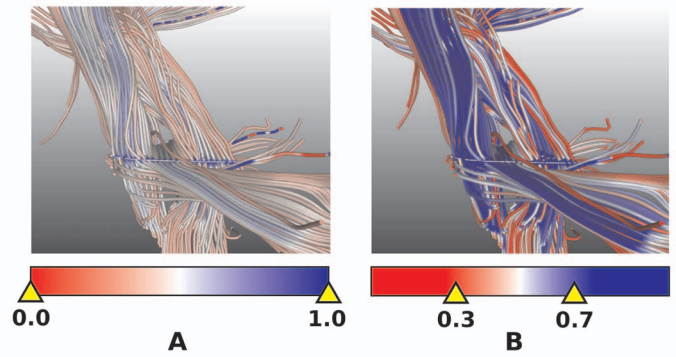


Fig. 7. (A) Color scale mapped to full threshold domain $[0, 1]$. (B) Color scale mapped to threshold region-of-interest $[0.3, 0.7]$. This highlights threshold variations along the fibers with full color detail.

comparative studies of white matter between patients, quantitative tract features are often used. It is important to verify whether a given tract feature is sensitive to threshold variations or not. The feature map view can be used specifically for this purpose. As mentioned previously each point in the threshold space corresponds to a single fiber tracking result. Section 4.2 discussed the different features that can be computed for such a tract. Obviously, we cannot compute a tract feature for each point in the threshold space because there are infinitely many of them. However, we can sample the space on a rectilinear grid and compute a tract feature for each sample point. We can then display the feature values as a 2D image where each sample point is represented by a pixel. We call this image the *feature map* and by using gray scale coloring we can highlight subtle changes in the tract feature values as a function of threshold combination. The user can select different features from a pull-down menu. We decided not to merge the feature map view with the color map view because the feature map itself would lose too much gray value contrast when combined with the RGB/HSV color maps. Instead, we provide the feature map as a separate view where you can optionally overlay the color map region of interest with a user-defined opacity.

Histogram Views: We provide several histograms as an alternative way of displaying threshold sensitivity. The threshold histograms were already discussed in Section 4.2, except here they are visualized as separate 1D histograms. They can be converted to cumulative histograms, which makes it easier to detect flat (and therefore stable) regions in the threshold space. We also show a feature histogram which is simply a histogram constructed from the list of feature values computed on the grid sample points described in the previous paragraph. The feature histogram shows the currently selected feature.

6 RESULTS AND DISCUSSION

In this section we present a number of visualizations that were created for three clinical DTI datasets. The first dataset represents a

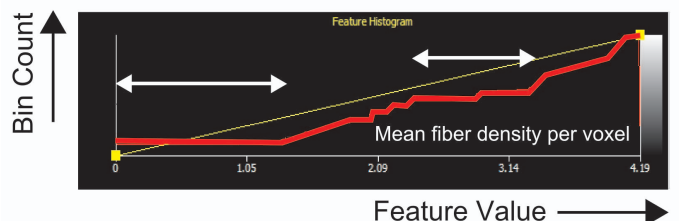


Fig. 8. Cumulative feature histogram (indicated by red line) for mean fiber density per voxel. The white arrows indicate areas where the tract feature is relatively stable for threshold variations.

healthy human brain (Siemens 3 Tesla, voxel dimensions $1 \times 1 \times 1$ mm³, resolution $231 \times 172 \times 131$, 72 directions). The second dataset also represents a healthy human brain (Philips 3 Tesla, voxel dimensions $2 \times 2 \times 2$ mm³, resolution $128 \times 128 \times 66$, 32 directions). The third dataset represents muscle tissue of a right human forearm (Philips 3 Tesla, voxel dimensions $1.79 \times 1.79 \times 6$ mm³, resolution $112 \times 112 \times 54$, 15 directions). Figure 10 illustrates how our visualization method can help find critical threshold variations along the streamlines. You can see a clear white band running across a group of neighboring streamlines (indicated by the white arrow). The colors sudden transition from blue through white to red corresponding to a sudden drop in the fractional anisotropy threshold. If this drop was purely caused by noise it would be unlikely to form such a regular, localized band pattern across multiple streamlines. Another phenomenon which our approach can help identify is crossing fiber structures. Figure 11 illustrates how a sudden drop in curvature threshold can result in the tracking of erroneous fiber tracts such as the cingulum, which runs along the “gutter” of the corpus callosum complex. Such a region may contain more disk-shaped tensors where the main diffusion direction not well-defined ($\lambda_1 \approx \lambda_2$). In this case, fiber tracking becomes very sensitive to noise and can start tracing the wrong tract. Using our tool, you can see exactly the point at which this wrong turn occurs. If you pick this location with the mouse, the exact threshold values will be indicated in the color map.

To further evaluate the added value of our visualization approach, we have asked three expert users to give feedback on the practical utility of our tool using these three datasets. All of them use DTI fiber tracking on a regular basis albeit for quite different research purposes. We performed the evaluation by first demonstrating the tool to the user. We then let the user work with the tool him or herself. After this, we presented the user with a list of questions designed to obtain structured feedback about the practical utility of our tool and parameter sensitivity visualization in general.

6.1 Brain Development in Premature Neonates

Our first user is a clinical physician who uses DTI fiber tracking to study the effect of hypoxic ischemia on white matter development in premature neonates. To show the difference between neonates with white matter deficiencies and healthy controls, this user uses quantitative tract-based features. However, because such features are highly dependent on stopping criteria, this has been problematic. In the past, our user investigated the sensitivity of stopping criteria on certain tract features by repeatedly performing fiber tracking with different combinations of thresholds. With existing DTI tools this is extremely time-consuming, so the possibility to show this information in a single featuremap of our tool was very much appreciated. Especially regions of the feature map that are relatively constant are of particular interest because they point to subranges of the threshold space where the feature is relatively stable and can be safely used for inter-subject comparison.

Typical tract features our user is interested in are tract volume and average fiber length. These are available in our tool. We briefly discussed the average fiber density per voxel feature. Our user is not using this feature at the moment but thought that it could be combined

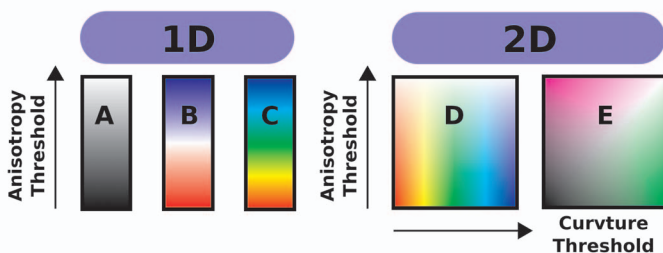


Fig. 9. 1D color maps: (A) gray scale, (B) red-white-blue, (C) rainbow. 2D color maps: (D) hue (rainbow)-saturation, (E) complementary colors (green-purple).

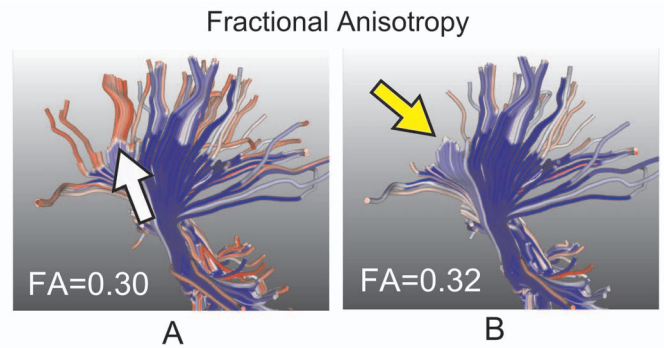


Fig. 10. Effect of small variations in anisotropy threshold on fiber tracts of the corona radiata (running from the brainstem towards the brain cortex). If fractional anisotropy is increased from 0.30 to 0.32 the red tract parts (indicated by yellow arrow) completely disappear (A + B). The cut-off point is already visible in Figure A in the white regions of the fibers (indicated by white arrow).

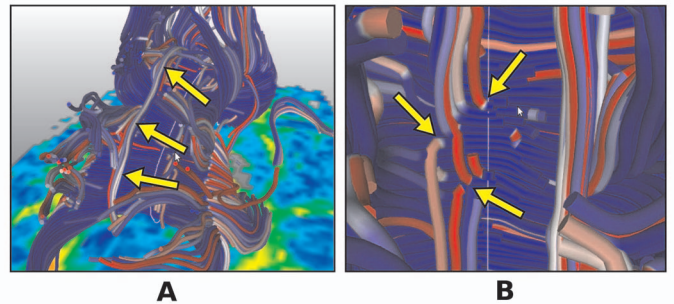


Fig. 11. (A) Reconstruction of the corpus callosum with unintended tracing of the cingulum (indicated by yellow arrows). (B) Close-up of area where unintended tracing originates. Color variations (blue to red with narrow band of white) show the sudden drop in curvature threshold which seems to be responsible for deviation of the pathway into the cingulum.

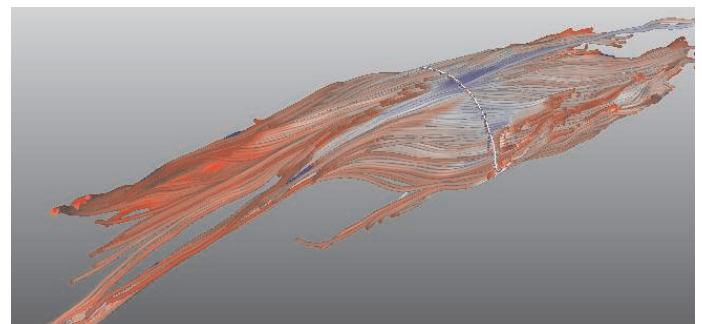


Fig. 12. Fiber tracking of muscle in human forearm. The elbow is located in the top-right corner, the hand is located in the bottom-left corner, palm facing upward. Red colored tissue are tendons running towards the hand. White colored tissue is muscle. The blueish colorations indicate attachment of muscle to bone.

with tract volume by weighting each voxel's contribution with its fiber density. Some feature that our user suggested to be included are the average anisotropy (either fractional or linear) along the fiber tract and the average apparent diffusion coefficient (ADC). We do not support these features at the moment but they can be easily included. Because so many different, application-specific tract features are available [9], we did not provide a complete list.

6.2 Muscle Tissue

Our second user is a researcher who uses DTI and fiber tracking methods to investigate injury and repair of muscle tissue. With DTI it is possible to detect subtle tissue differences that are not visible on normal MR. After demonstrating our visualization tool, we let the user interact with one of his own datasets. Showing DTI-based parameters along the streamlines is a feature that is completely missing in the tools our user is currently working with. He encouraged us to extend the number of parameters that can be shown along the streamlines (now we show only anisotropy and curvature thresholds) but even with just the anisotropy color coding he saw, for the first time in 3D, transitions from muscle tissue to connective tissue (tendons). Figure 12 illustrates these transitions (red = connective tissue, white = muscle, blue = bone attachment) for a selected set of muscles in the forearm.

We also discussed the various tract features with our user. He is particularly interested in tract volume and average fiber length because these, together with the attachment angle between muscle and bone, are sufficient to model the muscle for biomechanical simulations. However, since these features are highly dependent on user-defined stopping criteria, it is difficult to find values that are reproducible. Our visualization method was considered to be very useful for visualizing the variation of feature values as a function of stopping thresholds. Another feature that our user found interesting is the mean of end-point distances. Muscle fibers run highly parallel. As long as the fiber tracking output contains only muscle fibers, this feature is expected to remain relatively constant. However, when muscle fibers converge to form connective tissue the streamline end-points are expected to come closer together, resulting in a *decrease* of the mean of end-point distances. If the goal is to segment only muscle fibers, this can help to find the exact thresholds where muscle fibers move into connective tissue. The threshold histogram provides similar information because the anisotropy threshold of connective tissue is generally lower than muscle tissue. As soon as many connective fibers are being traced by the algorithm, a sudden jump in fiber length is expected which results in a peak in the threshold histogram. The average fiber density per voxel is expected to *increase* as muscle fibers converge to form more dense tendon fibers (show pictures of this).

The overall feedback of this user was very positive because our tool directly showed tissue transitions in 3D that had not been seen previously. The tract features we provided are by no means complete but the general approach of showing the behavior of any tract-based feature as a function of threshold was considered very useful, especially for group studies. Tract features are highly dependent on user settings however, which is why some people are reluctant to use them. Our user also strongly encouraged us to extend the parameter-space concept to other tensor-based properties such as the apparent diffusion coefficient and the tensor's main eigenvalue.

6.3 Brain Connectivity

Our third and last user is a researcher involved in the study of brain connectivity who uses DTI fiber tracking together with functional MR to investigate a patient with Landau-Kleffner syndrome. This patient acquired aphasia (loss of receptive and expressive language skills) due to epileptic seizures in the temporal lobe during early childhood. After more than 15 years of intensive training in sign language she is able to communicate quite well, although she has trouble understanding people without actually seeing them. The goal is to investigate whether she has formed brain connections that are not present in healthy controls. Especially connections between the remaining language areas and the motor area dealing with hand coordination are of interest. The main problem when using DTI fiber tracking for this type of research is finding threshold values that are sufficiently low to confirm a suspected connection between two regions of interest, but are also sufficiently high to be plausible. Our visualization was considered very useful in helping to make a more reliable choice of threshold values. As with the second user, this user suggested to extend the parameter space concept to include parameters that describe tensor shape. For example, it would have been interesting to show *linear* anisotropy threshold on one axis and *fractional* anisotropy threshold on the other axis. Using

2D color coding along the streamlines, you could then see where the tensor shape suddenly changes from linear to planar or vice versa. If this occurs at regular positions across multiple streamlines, this might point to true tissue changes (e.g., fiber crossing) instead of just noise. This user was rather sceptical about using tract-based features because of their sensitivity to user-defined parameters. We showed how our visualization method can be used to investigate how stable a tract feature really is within the range of threshold values relevant for the user's application. He agreed that our approach would encourage the use of quantitative tract features more often. They can provide additional information for showing that certain brain connections only exist in patients and not in healthy controls.

7 CONCLUSIONS AND FUTURE WORK

We have presented an approach for visualizing parameter sensitivity in DTI fiber tracking algorithms. To give a first impression and proof-of-concept of our method we focussed on the stopping criteria that determine when fiber tracking should terminate. We have shown that visualization of variations in the threshold values can give users insight into why streamlines terminate or follow erroneous pathways. This is relevant information for both brain scientists and neurosurgeons who are trying to assess whether their fiber tracking results can be relied upon. The use of tract-based features is indispensable for comparative studies of white matter development and disease. Being able to visualize their sensitivity for parameter variations is equally important because it provides the investigator with additional information to choose the most stable feature for the application. The feedback we received from our users confirms this point. Our tool allows the use of any scalar-based feature.

Parameter sensitivity is an aspect of visualization that is commonly ignored even though it can introduce considerable uncertainty in the output result. In this paper we have focussed on parameter sensitivity in DTI fiber tracking, however we wish to expand our research to include other sources of uncertainty regarding DTI and its applications. The DTI visualization pipeline involves many stages where uncertainties may be introduced. We wish to gain a better understanding of how these uncertainties propagate through the system and at which stages the greatest variability occurs. Other parameters that we wish to investigate are the effect of dataset resolution, but also other user-defined settings such as seed-point placement. The effect of noise on fiber tracking has already been investigated by others [15] but it would be interesting to look at the combination of noise-based variance with parameter sensitivity.

ACKNOWLEDGMENTS

The authors would like to thank Carola van Pul of the Maxima Medical Center of Eindhoven, Pim Pullens of BrainVoyager Maastricht and Martijn Froeling of the Technical University of Eindhoven for their help in evaluating our software. Also, Rainer Goebel of BrainVoyager Maastricht and Pieter Kubben, resident neurosurgeon at Maastricht Medical Center for supplying the datasets.

REFERENCES

- [1] D. Akers, A. Sherbondy, R. Mackenzie, R. Dougherty, and B. Wandell. Exploration of the Brain's White Matter Pathways with Dynamic Queries. In *Proceedings of IEEE Visualization '04*, pages 377–384, 2005.
- [2] P. Basser, J. Mattiello, and D. LeBihan. Estimation of the Effective Self-Diffusion Tensor From the NMR Spin Echo. *Journal of Magnetic Resonance*, 103:247–254, 1994.
- [3] P. Basser, S. Pajevic, C. Pierpaoli, J. Duda, and A. Aldroubi. In Vivo Fiber Tractography using DT-MRI Data. *Magnetic Resonance in Medicine*, 44:625–632, 2000.
- [4] C. Beaulieu. The Basis of Anisotropic Water Diffusion in the Nervous System. *NMR in Biomedicine*, 15:435–455, 2002.
- [5] J. Blaas, C. Botha, B. Peters, F. Vos, and F. Post. Fast and Reproducible Fiber Bundle Selection in DTI Visualization. In *Proceedings of IEEE Visualization '05*, pages 59–64, 2005.
- [6] R. Botchen, D. Weiskopf, and T. Ertl. Texture-Based Visualization of Uncertainty in Flow Fields. In *Proceedings of IEEE Visualization '05*, pages 647–654, 2005.

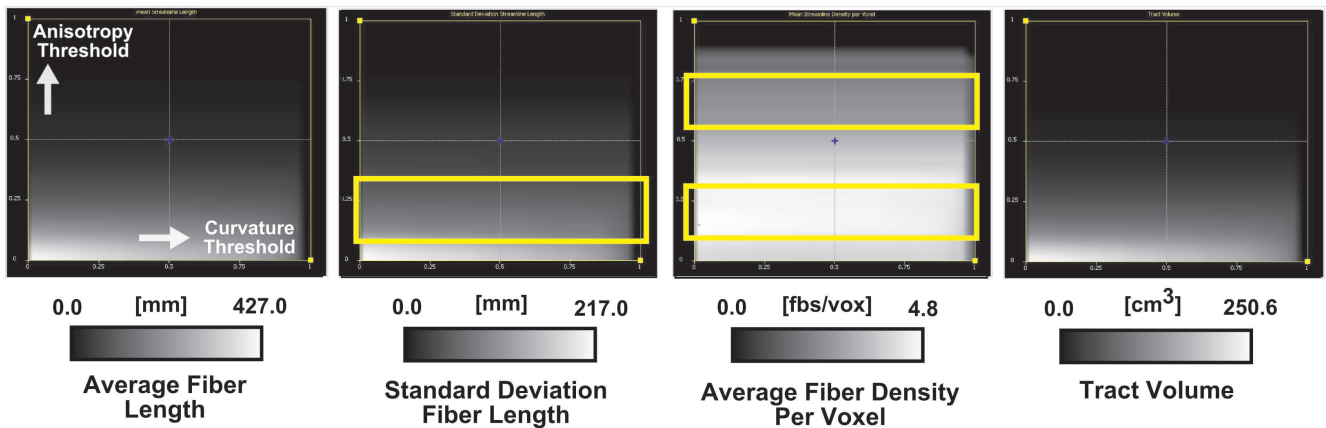


Fig. 13. Four example feature maps (anisotropy on vertical axis, curvature on horizontal axis). Average fiber length shows gradual increase as both the anisotropy and curvature thresholds become lower, indicating a strong dependency on these thresholds. Standard deviation of fiber length has a region of constant value (yellow box) where at least the anisotropy threshold seems to have little effect. Average fiber density per voxel has two regions that are relatively stable (yellow boxes). The tract volume feature also shows a significant dependence on anisotropy threshold variation. The color legends indicate the min/max range and unit of measurement for each feature.

- [7] O. Ciccarelli, G. Parker, A. Toosy, C. Wheeler-Kingshott, G. Barker, P. Boulby, D. Miller, and A. Thompson. From Diffusion Tractography to Quantitative White Matter Tract Measures - A Reproducibility Study. *NeuroImage*, 18:348–359, 2003.
- [8] T. Conturo, N. Lori, T. Cull, E. Akbudak, A. Snyder, J. Shimony, R. McKinstry, H. Burton, and M. Raichie. Tracking Neuronal Fiber Pathways in the Living Human Brain. In *Proceedings of National Academy of Sciences (PNAS '99)*, pages 10422–10427, 1999.
- [9] S. Correia, S. Lee, T. Voorn, D. Tate, R. Paul, S. Zhang, S. Salloway, P. Malloy, and D. Laidlaw. Quantitative Tractography Metrics of White Matter Integrity in Diffusion-Tensor MRI. *NeuroImage*, 42:568–581, 2008.
- [10] H. Doleish, M. Gasser, and H. Hauser. Interactive Feature Specification for Focus+Context Visualization of Complex Simulation Data. In *Proceedings of Symposium on Data Visualization '03*, pages 239–248, 2003.
- [11] J. Eyton. Complementary-Color Two-Variable Maps. *Annals of the Association of American Geographers*, 74:477–490, 1984.
- [12] G. Grigoryan and P. Rheingans. Point-Based Probabilistic Surfaces to Show Surface Uncertainty. *IEEE Transactions on Visualization and Computer Graphics*, 10:564–573, 2004.
- [13] M. Hadwiger, L. Fritz, C. Rezk-Salama, T. Hoell, G. Geier, and T. Pabel. Interactive Volume Exploration for Feature Detection and Quantification in Industrial CT Data. In *Proceedings of IEEE Visualization '08*, pages 1507–1514, 2008.
- [14] D. Jones. Determining and Visualizing Uncertainty in Estimates of Fiber Orientation from Diffusion Tensor MRI. In *Proceedings of International Society for Magnetic Resonance Medicine (ISMRM '02)*, volume 49, pages 7–12, 2003.
- [15] D. Jones and C. Pierpaoli. Confidence Mapping in Diffusion Tensor Magnetic Resonance Imaging. In *Proceedings of International Society for Magnetic Resonance Medicine (ISMRM '05)*, volume 53, pages 1143–1149, 2005.
- [16] M. Lazar and A. Alexander. An Error Analysis of White Matter Tractography Methods - Synthetic Diffusion Tensor Field Simulations. *NeuroImage*, 20:1140–1153, 2003.
- [17] S. Lodha, A. Pang, R. Sheehan, and C. Wittenbrink. UFLOW: Visualizing Uncertainty in Fluid Flow. In *Proceedings of IEEE Visualization '96*, pages 249–254, 1996.
- [18] C. Lundstroem, P. Ljung, A. Persson, and A. Ynnerman. Uncertainty Visualization in Medical Volume Rendering Using Probabilistic Animation. *IEEE Transactions on Visualization and Computer Graphics*, 13:1648–1655, 2007.
- [19] B. Moberts, A. Vilanova, and J. v. Wijk. Evaluation of Fiber Clustering Methods for Diffusion Tensor Imaging. In *Proceedings of IEEE Visualization '05*, pages 65–72, 2005.
- [20] S. Mori, B. Crain, V. Chacko, and P. v. Zijl. Three Dimensional Tracking of Axonal Projections in the Brain by Magnetic Resonance Imaging. *Annals of Neurology*, 45:265–269, 1999.
- [21] S. Mori and P. v. Zijl. Fiber Tracking - Principles and Strategies. *NMR in Biomedicine*, 15:468–480, 2002.
- [22] A. Pang, C. Wittenbrink, and S. Lodha. Approaches to Uncertainty Visualization. *The Visual Computer*, 13:370–390, 1997.
- [23] C. Pierpaoli and P. Basser. Toward a Quantitative Assessment of Diffusion Anisotropy. *Magnetic Resonance in Medicine*, 36:893–906, 1996.
- [24] P. Rheingans. Task-Based Color Scale Design. In *Proceedings of Applied Image and Pattern Recognition (SPIE '99)*, pages 35–43, 1999.
- [25] S. Silva, J. Madeira, and B. Santos. There is More to Color Scales Than Meets the Eye - A Review on the Use of Color in Visualization. In *Proceedings of Information Visualization '07*, pages 943–950, 2007.
- [26] T. Taoka, M. Morikawa, T. Akashi, T. Miyasaka, H. Nakagawa, K. Kiyuchi, T. Kishimoto, and K. Kichikawa. Fractional anisotropy - threshold dependence in tract-based diffusion tensor analysis: Evaluation of the uncinate fasciculus in alzheimer disease. *American Journal of Neuro-radiology*, 2009.
- [27] A. Vilanova, S. Zhang, G. Kindlmann, and D. Laidlaw. *Visualization and Image Processing of Tensor Fields*, chapter An Introduction to Visualization of Diffusion Tensor Imaging and Its Applications, pages 121–153. Mathematics and Visualization. Springer Verlag, 2004.
- [28] S. Wakana, A. Caprihan, M. Panzenboeck, J. Fallon, M. Perry, R. Gollub, K. Hua, J. Zhang, H. Jiang, and P. Dubey. Reproducibility of Quantitative Tractography Methods Applied to Cerebral White Matter. *NeuroImage*, 36:630–644, 2007.
- [29] X. Wei, A. Kaufman, and T. Hallman. Case Study: Visualization of Particle Track Data. In *Proceedings of IEEE Visualization '01*, pages 465–468, 2001.
- [30] F. Weiler, H. Hahn, A. Koehn, O. Friman, J. Klein, and H.-O. Peitgen. Dealing with Inaccuracies in Multimodal Neurosurgical Planning - A Preliminary Concept. In *Proceedings of the 22nd Internal Congress and Exhibition of Computer Assisted Radiology and Surgery (CARS) 2008*, 2008.
- [31] D. Weinstein, G. Kindlmann, and E. Lundberg. Tensorlines - Advection-Diffusion Based Propagation Through Diffusion Tensor Fields. In *Proceedings of IEEE Visualization '99*, pages 249–254, 1999.
- [32] A. Wenger, D. Keefe, S. Zhang, and D. Laidlaw. Interactive Volume Rendering of Thin Thread Structures within Multivalued Scientific Data Sets. *IEEE Transactions on Visualization and Computer Graphics*, 10:664–672, 2004.
- [33] C. Wittenbrink, A. Pang, and S. Lodha. Glyphs for Visualizing Uncertainty in Vector Fields. *IEEE Transactions on Visualization and Computer Graphics*, 2:266–279, 1996.